STRONG GEOMAGNETIC STORMS AND GLOBAL SEISMIC ACTIVITY OF THE EARTH

© 2025 V. V. Hegai*, A. D. Legenka**

Pushkov Institute of Terrestrial Magnetism, Ionosphere, and Radio Wave Propagation (IZMIRAN), Moscow, Troitsk, Russia

**e-mail:* hegai@izmiran.ru

***e-mail:* leg@izmiran.ru

Received February 06, 2025

Revised March 27, 2025

Accepted May 22, 2025

Abstract. An analysis of the global seismic Earth′s activity has been carried out in order to identify the possible impact of strong magnetic storms on it. In its analysis, the initial quantitative measure of the global Earth's seismic activity the total number of strong (magnitude $M \geq 5.0$) crustal (hypocenter depth $0 \leq h \leq 60$ km) earthquakes worldwide per day (N_{EQ}) have been selected. The geomagnetic activity and strength of each specific magnetic storm were estimated based on the hourly values of the *DST*-index. Only strong geomagnetic storms that met the condition $DST_{extr} \leq$ –150 nT were considered, and only those for which there are the final data on hourly values of the *DST*-index were included in the studied array of storms (for the period from 1957 to 2016). A modified epoch superposition method was used as the main analysis tool, while the day on which the minimum value of the *DST*-index was reached was considered the reference (zero) day.
It was found that the day before the reference day (on minus 1st day), there is a significant decrease in global seismic activity of the Earth for sudden onset magnetic storms (MS_{SC}). On day zero, the situation is not so clear, but there is a definite increase in global seismic activity of the Earth for magnetic storms with a gradual onset (MS_{GRAD}). Moreover, on the +7th day for such storms, there is a significant increase in the seismic activity of the Earth. Possible physical mechanisms are proposed and discussed to explain this behavior of global seismic activity of the Earth based on extremely simplified quantitative estimates.

Keywords: *strong geomagnetic storms, global seismic activity of the Earth*

DOI: 10.31857/S00167940250516e9

1. INTRODUCTION

Systematic studies of the possible connection between magnetic storms and earthquakes have been carried out for quite a long time (see an overview of the problem in [Sytinsky, 1973; 1989]). In a cycle of works [Sobolev et al., 1998; 2001; Zakrzhevskaya and Sobolev, 2004; Sobolev, 2021], the authors confirm the impact of magnetic storms on the Earth's seismic activity and tectonic deformations, as well as on the low-frequency seismic noise [Sobolev et al., 2020].

However, the geophysical literature continues to actively discuss the possibility of trigger effects of geomagnetic storms caused by solar activity on the Earth's seismicity. Thus, relatively recently, in [Kozyreva and Pilipenko, 2020], the authors tried to test the idea of a magnetic storm and its induced telluric fields and currents as an earthquake trigger for Alaska, a region with high seismicity and strong magnetic activity. In this work, they examined the statistics of geomagnetic variations at College Station (USA) before and after the 2014-2016 surface (crustal) earthquakes using the superimposed epoch method for median values of magnetic perturbation relative to the earthquake moment. Their results did not support the hypothesis of magnetic storm and substorm as possible earthquake triggers for the Alaska region. However, the authors suggested that their work should not be viewed as a final verdict, but as an invitation to cosmophysicists and seismologists to jointly discuss trigger seismicity. In response to this invitation, a paper [Guglielmi, 2020] was published in the same year. In it (contrary to the conclusions of the authors of [Kozyreva and Pilipenko, 2020]), the papers were named in which the connection of seismicity with magnetic disturbances and other exogenous factors was found at a statistically significant level. The same paper [Guglielmi, 2020] suggested the reason why the authors of [Kozyreva and Pilipenko, 2020] did not find evidence of such a connection.

Our paper continues the discussion on the indicated topic. It will also use a slightly modified method of epoch superposition, in which not the moment of the earthquake, but the day (zero!) on which the extremely low value of the *DST-index* during a particular geomagnetic storm (DST_{extr}) is reached, will serve as a reference.

Our study had two objectives. First, to obtain, on sufficiently large (but limited) statistics, quantitative estimates on the basis of which it will be possible to judge possible physical mechanisms of the relationship between the Earth's global seismic activity (SAZ) and geomagnetic storms. Second, to carry out our own extremely simplified quantitative assessments for the proposed mechanisms of such coupling, and to consider in the appropriate context one of the already available model assessments carried out in [Trenkin, 2015].

2. CONDITIONS OF DATA SELECTION, THEIR SOURCES AND METHOD OF ANALYSIS

For the analysis of possible changes in the global SAZ due to geomagnetic storms, we selected an array of storms from 1957 to 2016, for which the final data of hourly DST-index values for each month are available in the catalog of the World Data Center for Geomagnetism, Kyoto (https://wdc.kugi.kyoto-u.ac.jp/). In addition, an additional restriction on the geomagnetic storm intensity was imposed: only strong magnetic storms meeting the DST_{extr} condition≤ -150 nTL were considered. These magnetic storms (according to the classification given in the study [Loewe and Prölss, 1997]) are classified as Strong (Strong: $DST \in$ [-100, -200) nTl), Very Strong (Severe: $DST \in$ [-200, -350) nTl), and Extreme (Great: | DST| ≥ 350 nTl).

It should be noted at once that the impact on the Earth's magnetosphere of magnetic storms with gradual onset (MS_{GRAD}) differs significantly from the impact on the same magnetosphere of magnetic storms with sudden onset (MS_{SC}). This is due to the fact that (as shown in [Obridko et al., 2013]) they are associated with different agents on the Sun and, therefore, form independent of each other and uncorrelated populations.

First of all, this difference is characteristic of the magnetospheric compression rate under the pressure of the perturbed solar wind. Thus, in [Kalegaev and Nazarkov, 2016], the dynamics of the magnetosphere during the development of a geomagnetic storm with a gradual onset (February 14, 2009) was considered. In particular, the authors point out that the beginning of this magnetic storm corresponds to the time of 02:00 h UT, when the magnetosphere compression by the perturbed solar wind begins. At the same time, an amplification of the Chapman-Ferraro currents at the magnetopause was recorded, which reached a maximum according to the DST-index values around 05:35 UT. At 06:00 UT of the same day, the B_z-component of the interplanetary magnetic field (IMF) changed its direction from northern to southern. The main phase of the storm began, during which the minimum of the *DST* index was recorded by at about 10:00 UT. From this description of the authors it follows that the magnetospheric compression occurred in the interval from 02:00 UT to 05:35-06:00 UT and lasted for 3.5-4 h.

Another characteristic time of magnetospheric compression is observed when considering the evolution of a magnetic storm with a sudden onset. It, as will be shown below, can be of the order of tens of minutes. A detailed analysis of the magnetospheric behavior for two storms with sudden onset (MS_{SC}) is given in [Kalegaev et al., 2015]. We will use the description of the authors of this paper for the storm of January 21-22, 2005 with a sudden onset. The authors indicate that the coronal mass ejection (CME) led to a strong compression of the Earth's magnetosphere on January 21, 2005. The distance to the sunspot decreased to ~ $6R_W$, and this compression occurred within 20 min, from 17:00 UT to 17:20 UT. At the same time, the *SYM_H* index (analogous to the DST *index*, but with minute resolution) changed from -17 nTL to 51 nTL, indicating a significant enhancement of the Chapman-Ferraro currents at the magnetopause.

In accordance with the above, we first formed an array of 128 storms (*128MS*) from the catalog of geomagnetic storms (https://www.izmiran.ru/magnetism/magobs/MagneticStormCatalog.html), consisting of two parts: array ($86MS_{SC}$) - storms with a sudden onset and array ($42MS_{GRAD}$) - storms with a gradual onset. As can be seen, the number of magnetic storms in the array ($42MS_{GRAD}$) is about half the number in the array ($86MS_{SC}$). This is due to the fact that storms with gradual onset of high intensity are generally fewer than storms with sudden onset of the same intensity.

Further, the number of strong (with magnitude $M \geq 5.0$) crustal (hypocenter depth $0 \leq h \leq$ 60 km) earthquakes per day (N_{EQ}) around the world was taken as a baseline measure of global $_{EMS}$ intensity. A detailed justification for this choice is given in [Hegai et al., 2022a]. Daily (or hourly) data on earthquakes can be obtained from the catalog of the National Earthquake Information Center of the U.S. Geological Survey (NEIC, USGS, see the site (https://www.usgs.gov/)).

Data on the number of earthquakes per day (N_{EQ}) around the world were processed using the method of epoch superposition (for a description of the method, see, for example, the monograph [Chizhevsky, 1976], and its adaptation for the solution of modern geophysical problems - the work [Desherevsky and Idarmachev, 2024]) as follows: over a seventeen-day interval (starting from the -8th day to the +8th day), the ensemble of realizations of daily $N_{(EQ)}$ values for the selected array of geomagnetic storms is averaged. The zero (reference) day is considered to be the day on which the minimum of the *DST-index* for each individual storm of the selected array is reached. Thus, as already mentioned in the INTRODUCTION, the reference is made not to the moment of the earthquake, but to the day of *the DST-index* minimum on the selected 17-day interval. The results of this processing are summarized in the next section.

3. RESULTS

Figure 1 shows the ensemble-averaged values of $\langle N_{EQ} \rangle$ over the 17-day interval (solid lines with dots) obtained by the method of overlapping "epochs", with the zero day taken as the one on which the minimum value of the *DST-index* is reached. Panel a -$\langle N_{EQ} \rangle$ for the ensemble of all selected 128 geomagnetic storms (*128MS*); panel *b* -$\langle N_{EQ} \rangle$ for the group of 86 geomagnetic storms with sudden onset ($86MS_{SC}$) included in this ensemble; panel *c* -$\langle N_{EQ} \rangle$ for another group of 42 geomagnetic storms with gradual onset ($42MS_{GRAD}$) included in the full ensemble. The solid straight lines in the panels indicate the mean values (MEAN$\langle N_{EQ} \rangle$) over the indicated time interval, and the dashed straight lines indicate the scatter bands of MEAN$\langle N_{EQ} \rangle \pm 2\sigma$, where σ is the standard (standard deviation). The solid "circles" in the figure show the exit of the values $\langle N_{EQ} \rangle$ outside the scatter band, and the "circle" given by the dashed line is for the value $\langle N_{EQ} \rangle$, approaching the upper limit of the scatter as close as possible (panel *c*, day zero).

Fig. 1.

A comparison of panels (*a*) and (*b*) shows that the decrease of the SAS for the full ensemble of magnetic storms (*128MS*, panel *a*) on day -1 by -19.9% relative to MEAN$\langle N_{EQ} \rangle$ with simultaneous exceeding the boundary of the MEAN$\langle N_{EQ} \rangle$ - 2σ level by -1.5% relative to it is significantly aggravated for the *86MS*$_{SC}$ group (panel *b*). The decrease in the SAS reaches already -28% of MEAN$\langle N_{EQ} \rangle$, and the output beyond the MEAN$\langle N_{EQ} \rangle$ - 2σ level boundary is -7.5%, i.e. it increases 5-fold in absolute value. At the same time, the consideration of panel *c*, i.e., another group of storms (with gradual onset, *42MS*$_{GRAD}$) shows a slight decrease in the NAD on day -1 relative to MEAN$\langle N_{EQ} \rangle$.

Thus, for the selected array of magnetic storms, we can conclude that storms with sudden onset (*86MS*$_{SC}$) are characterized by a significant decrease in the SAS on the day preceding the day on which the minimum value of the *DST index* is reached (*DST*$_{extr}$).

To the best of the authors' knowledge, this kind of result was first presented in [Guglielmi et al., 2015] and was obtained on a much larger statistical material. The authors of this work performed a comparative analysis of seismicity at intervals of ±60 min relative to the SSC (storm sudden commencement - SSC or SC, see in particular the corresponding definition on the website (http://www.wdcb.ru/stp/geomag/geomagnetic_storms.html)). They found with a high degree of certainty that the number of earthquakes is noticeably greater before the SSC than after the SSC. The authors point out, "In other words, the SSC suppresses global seismicity." and, further, "We are not inclined to exaggerate the cognitive value of the established link between the SSC and earthquakes. Indeed, the description of any empirical relationship is only a necessary step toward understanding, i.e., ultimately toward the construction of a physical and mathematical model of a natural phenomenon. But no theoretical interpretation of the relationship between SSC and earthquakes has been found so far. We consider this situation rather critical, so further research is needed in the hope of finding the key to solving an interesting and important problem."

In our independent study it turns out, first, that this result is confirmed. At the same time, there is an extension of the hour interval to days, during which the SCA is significantly reduced for magnetic storms with sudden onset. This is probably due to the fact that the SC momentum is randomly distributed within a day in our approach. Secondly, we will return to the issue of constructing a physical and mathematical model of possible processes to explain such a situation in Section 4 below.

Fig. 2.

Here, as an illustration, we present Fig. 2, which is a copy of panel *b* of Fig. 1, but with a resolution of 1 hour on the time interval from -2 to +2 days. The notations on it are similar to Fig. 1, and the MEAN⟨N_{EQ}⟩ $86MS_{SC}$ and standard deviation σ are calculated for this five-day interval.

It is well seen that the values of ⟨N_{EQ}⟩ $86MS_{SC}$ on day -1 are only three times above the MEAN⟨N_{EQ}⟩ $86MS_{SC}$ line and nowhere above the level of MEAN⟨N_{EQ}⟩ $86MS_{SC}$ + σ, whereas on all other days this level is exceeded many times, even more so the level of MEAN⟨N_{EQ}⟩ $86MS_{SC}$.

Let us now return again to Fig. 1 (panel *c*) for the group of magnetic storms with gradual onset $42MS_{GRAD}$. Two maxima in the behavior of ⟨N_{EQ}⟩ are noteworthy. The first one occurs on day 0 and exceeds the MEAN⟨N_{EQ}⟩ $42MS_{GRAD}$ level by 22.4%, approaching the MEAN⟨N_{EQ}⟩ $42MS_{GRAD}$ +2σ boundary ("circle" is shown by the dashed line). The second one is observed on day +7 ("circle" is shown as a solid line), exceeds the MEAN⟨N_{EQ}⟩ $42MS_{GRAD}$ level by 33.7% and lies above the MEAN⟨N_{EQ}⟩ $42MS_{GRAD}$ +2σ boundary by 5.5% of its value. This implies a significant increase in the NEA on day zero and a very significant increase on day +7 for the group of geomagnetic storms with a gradual onset of $42MS_{GRAD}$.

We also point out here that Δ[-1;0]*128MS* is the magnitude of the jump ⟨N_{EQ}⟩ between the values at day -1 and day zero ≅ 0.7 for the entire *128MS* magnetic storm ensemble, Δ[-1;0]$86MS_{SC}$ ≅ 0.71 for the $86MS_{SC}$ group , Δ[-1;0]$42MS_{GRAD}$ ≅ 0.67 for the $42MS_{GRAD}$group, and, respectively, Δ[+6;+7]$42MS_{(GRAD)}$≅0.71.

Further analysis of the $86MS_{SC}$group of geomagnetic storms was carried out according to the following feature: only those for which $\Delta T_{DSTextr}$ (the time interval between the maximum value of the *DST-index* before the beginning of the main phase of the geomagnetic storm, DST_{max}, and the time of reaching the value of its minimum value, DST_{extr}) did not exceed 24 h, i.e. $\Delta T_{DSTextr} \leq$ 24 h were selected from the entire group. Such magnetic storms turned out to be 60 ($60MS_{SC}$). The result of the analysis is presented in Fig. 3.

Fig. 3.

As can be seen from the comparison of Fig. 3 with Fig. 1 (panel *b*), day -1 also saw both a decrease in the MEAN⟨N_{EQ}⟩ $60MS_{SC}$ value at ≅ -31.3% of its value (compared to -28%) and an increase in the absolute value of the deviation from the -2σ level boundary, which amounted to -8.1% (compared to the previous value of -7.5%). This testifies in favor of the fact that for magnetic storms with a sudden onset with a short development phase, the decrease of the SAZ is more noticeable. There was also an increase in the magnitude of the SAZ jump: Δ[-1;0]$86MS_{SC}$ ≅ 0.71, and Δ[-1;0]$60MS_{SC}$ ≅ 0.73.

The results of the study of the $42MS_{\mathrm{GRAD}}$ array of magnetic storms with gradual onset by dividing it into two groups (group I: 19 storms for which $\Delta T_{DSTextr} > 24$ h and group II: 23 storms for which $\Delta T_{DSTextr} \leq 24$ h) are shown in Fig. 4.

Fig. 4.

From Fig. 4 (panel *b*) shows that it is the storms with gradual onset from group I ($\Delta T_{DSTextr} > 24$ h) that lead to a significant increase in the SAZ on day +7, while storms with gradual onset from group II ($\Delta T_{DSTextr} \leq 24$ h) give the most noticeable contribution to the SAZ intensity on day zero. The quantitative characteristics are as follows: for group I, the magnitude of $\langle N_{\mathrm{EQ}}\rangle$ on day +7 is 61% higher than MEAN$\langle N_{\mathrm{EQ}}\rangle$ $19MS_{\mathrm{GRAD}}$ and exceeds the MEAN$\langle N_{\mathrm{EQ}}\rangle$ $19MS_{(\mathrm{GRAD})}$ +2σ level by≅ 8.8% of its magnitude, and the spike in SAS Δ[+6;+7]$19MS_{\mathrm{GRAD}}$≅ 1.26; for group II, the value of $\langle N_{\mathrm{EQ}}\rangle$ on day zero is 27.8% higher than MEAN$\langle N_{\mathrm{EQ}}\rangle$ $23MS_{\mathrm{GRAD}}$and approaches MEAN$\langle N_{\mathrm{EQ}}\rangle$ $23MS_{\mathrm{GRAD}}$+2σ at≅ 96% of its value, and the jump in global SAS Δ[-1;0]$23MS_{\mathrm{GRAD}}$ ≅ 1.13.

4. DISCUSSION: HYPOTHETICAL PHYSICAL MECHANISMS OF THE GLOBAL SAS CONNECTION WITH MAGNETIC STORMS, EXTENDED ANALYSIS OF OBSERVATIONAL PROCESSING DATA, AND DISCUSSION OF THE RESULTS

First of all, we note here that the authors realize the hypothetical nature of a number of statements made in this section and the corresponding interpretation, but such a discussion seems quite justified and necessary in order to clarify the connection of the SAS with magnetic storms, which is why the present work is sent to the Discussion section of the Journal of Geomagnetism and Aeronomy.

4.1 The decrease of the SAS on the day preceding the day of DSTextr

The following hypothesis can be considered as a physical mechanism for the marked decrease in Earth's seismic activity (EAS) on the day preceding the extremely low value of the *DST index* during a geomagnetic storm with sudden onset (MS_{SC}). It is related to a rapid decrease of the magnetospheric volume due to its sharp compression under the influence of the accelerated and compacted matter of the perturbed solar wind during the initial period of the geomagnetic storm with a sudden onset (SC). As a result, the gas pressure increases in the reduced volume, which leads to the decrease of the SAZ.

Let us carry out an appropriate extremely simplified evaluation of this hypothesis based on the input parameters for this evaluation taken from the literature. Before the main phase of a strong magnetic storm with a sudden onset at its initial stage, the magnetosphere is sharply compressed under the action of an incoming shock wave in the perturbed solar wind (see, for example, (http://www.kaf07.mephi.ru/eduroom/appNuCosm/L8-1.pdf)). At the same time, the distance from the Earth's center to the sunward point of the magnetosphere boundary R (magnetopause) along the x-axis on the line Earth− Sun in the framework of the paraboloidal model of the magnetosphere (see, in particular, [Alexeev et al., 2001]) changes. Thus, during the magnetic storm 10− January 11, 1997, this distance decreased from $R_0 \cong 10R_E$ to $R_1 \cong 7R_E$. At the same time, the radius of the perpendicular to the *x-axis* paraboloid segment r (on the flank of the magnetosphere) at the point $x = 0$ (the Earth's center) changed from $r_0 \cong 15R_E$ to $r_1 \cong 10R_E$ (see (https://geo.phys.spbu.ru/magnetosphere/STPpracticum2005/P3_Korovinskiy/geoeffective_str.html)). The volume of a segment of a paraboloid of rotation (V) is given by the formula $V = \pi r^2 R/2$, so there has been a reduction in volume $V_0/V_1 = (r_0/r_1)^2(R_0/R_1) \cong 3.21$ by more than a factor of three. In the case of adiabatic contraction of the volume of ideal gas occupying this volume, the product of pressure (P) over volume (V) satisfies the relation $PV^\gamma = \text{const}$, with $\gamma = 1.4$. Then the pressure in the volume will increase in $P_1/P_0 = (V_0/V_1)^\gamma \approx 5$ times.

Of course, this assessment is very simplified, since the near-Earth plasma cannot be represented only as a gas subjected to compression at the time of a strong geomagnetic storm with a sudden onset. Nevertheless, experimental evidence of a sudden increase in the atmospheric pressure at the Earth's surface during geomagnetic perturbations was already given in [Ivanov and Semenov, 1990], where the possibilities of interpreting these increases in atmospheric pressure within the framework of hydrodynamic transmission mechanisms from the upper atmosphere were proposed. The results of [Morozova and Pudovkin, 2001] are also in favor of this scenario. In it, the variations of surface atmospheric pressure for 223 meteorological stations of the former USSR associated with solar proton events (SPEs) and Forbush decreases in the intensity of the flux of galactic cosmic rays (GCRs) were analyzed using the method of superimposed epochs. The entire region under consideration was divided into several synoptic zones on the basis of the type of pressure variations. The analysis of the obtained data showed that the character of atmospheric pressure variations caused by SPE and (or) Forbush-decreases of GCR depends on the geographical location of the weather station and the climatic zone in which it is located. In addition, it was found that after the SPE, the atmospheric pressure perturbations propagate predominantly in the latitudinal direction, and after the Forbush decreases - predominantly in the meridional directions.

Here it is necessary to note the following. At Forbush-decreases of GCR, in fact, the intensity of the GCR flux at the troposphere level decreases and, accordingly, the energy inflow and ionization in the lower atmosphere (height range 0− 25 km, the center of the layer at the height

~ 10 km) decrease. In the case of PCA, on the contrary, ionization and energy inflow increase in the layer lying in the height range 27− 65 km (layer center at ~ 40 km height, see [Mironova et al., 2015], Fig. 1). This can explain the difference in the changes in the atmospheric circulation regime in the troposphere at Forbush depressions of the GCR and SPS. Accordingly, the characteristic times of its restructuring, formation/destruction and evolution of the main baric structures in the troposphere - cyclones, anticyclones and troughs forming the cloud field - will also differ.

Thus, variations of the magnetosphere volume and pressure inside it (including near the Earth's surface) associated with strong geomagnetic storms appear to be synchronized with the circulation processes in the lower atmosphere and the movement of its main baric structures (baric troughs, cyclones, typhoons, hurricanes, and anticyclones). These same variations essentially determine the characteristic times of the surface circulation and pressure restructuring, since the magnetopause is the upper boundary of the separated volume of the surface plasma and the lower atmosphere, respectively, is the lower boundary. This factor is one of those that determine the intensity of the global SAZ during the development of strong geomagnetic storms.

4.2 Increase of the SAZ on the DST_{extr} day

The physical mechanism that initiates (already prepared by endogenous processes inside the Earth foci) earthquakes on the DST_{extr} day may be the Ampere force and its time derivative, which change in the interaction of three-dimensional current systems of the magnetosphere (first of all, the ring current I_{Ring} during strong magnetic storms) with the currents of the liquid inner core of the Earth (I_{Earth}), creating its main magnetic field. This interaction force reaches its maximum at the moment when the value of the *DST-index* is minimal during a magnetic storm and is equal to DST_{extr}. Our elementary estimates show that the interaction force of the ring current I_{Ring}, flowing in the magnetosphere in the toroidal region around the Earth with the center in its equatorial plane and at altitudes above the Earth's surface from ~ 10000 to 60000 km (i.e., ~ $2.6R_{\mathrm{Earth}}$- $10R_{\mathrm{Earth}}$ from its center) against the direction of its rotation (see, e.g., [*Daglis*, for example, work [Daglis, 2006]) with the current I_{Earth} increases about 10 times at the moment of maximum intensity of a strong magnetic storm. It is this force (and its temporal derivative) that could serve as a trigger for "ripe" earthquake sources, and it is greatest in the near-equatorial regions of the Earth (about $\pm 35^{\circ}$ in latitude, approximately being a projection of the toroidal region around the Earth's equator where the ring current is mainly concentrated), where the bulk of strong crustal earthquakes occurring on the Earth (see [Levin et al, 2013; Hegai et al., 2022b]). In our extremely simplified model scheme, we do not consider the system of Chapman− Ferraro currents flowing at the magnetopause. These currents flow in the direction opposite to the ring current, intensify at the beginning of a magnetic storm, and therefore also contribute to the shift of the intensifying ring current contour toward the Earth (also under the influence of the Ampere force).

However, according to other elementary estimates, a comparison of the Ampere force per unit area with the magnitude of the pressure acting at the upper boundary of the liquid core of the Earth shows that it is smaller than the latter by many orders of magnitude, which leads to very pessimistic conclusions regarding the effectiveness of such a mechanism.

Then there remains only the purely empirical fact that the DST_{extr} day is synchronized with the increase of the SAZ for short magnetic storms with a gradual onset ($\Delta T_{DSTextr} \leq 24$ h), which requires some physical explanation. Such an explanation is proposed in [Trenkin, 2015], in which a physical model of the impact of telluric currents on the processes of macrofracture formation in the Earth's crust and earthquake initiation due to the interaction of telluric currents with the geomagnetic field is proposed. According to this model, due to the reduction of electrical resistance in the future macrofracture, a significant part of the electrotelluric current will flow along the contour, partially or completely including the area of the forthcoming macrofracture. As a result of calculations carried out on this model, the author concludes: "Thus, the realization in the geophysical environment of the earthquake source values of telluric currents, providing, due to the Ampere force, the pressure sufficient to destroy geological structures, seems to be quite acceptable." Hence, the Ampere force in this context may still be the trigger of a crustal earthquake. It also follows from the model, "... that provided that the pending sources are located in the area of intense variations of the geomagnetic field and, consequently, in the field of magnetotelluric currents, additional pressure will "automatically" be applied to the areas of pending earthquakes. In the case of global geomagnetic disturbances, the model allows, in particular, to explain the observed episodes of synchronization of seismic flows in territories significantly separated in space."

4.3 Detailed discussion of the results

Let us now consider in more detail the results obtained in Section 3. For short magnetic storms with a gradual onset (see Fig. *4c*), there is no significant decrease in the SAZ on day -1 compared to the previous day (the magnetospheric compression is quite gradual, the volume decreases gradually, and there is no sharp increase in the pressure inside it), but there is a significant increase in the SAZ on day zero. As follows from the scenario proposed in [Trenkin, 2015], the intensification of telluric currents, if it coincides with the rate of amplification of the annular current, can lead to a corresponding increase in the SAZ.

Fig. 5.

In favor of such a scenario, the data presented in Fig. 5. It shows the geographical positions (circles) of the earthquake epicenters of all earthquakes on day zero for the array of short geomagnetic storms with gradual onset ($23MS_{GRAD}$, $\Delta T_{DSTextr} \leq 24$ h). The figure shows that all epicenters are located in the band of geographic latitudes ±35° relative to the equator, i.e., in the area of projection of the "torus" of the ring current encompassing the Earth onto its surface.

Fig. 6.

Fig. 6 shows a similar picture to Fig. 5, but only for long geomagnetic storms with a gradual onset (*19MS*GRAD, for which $\Delta T_{DSTextr} > 24$ h) on day +7, the SAZ for which is shown in panel (*b*) of Fig. 4 in Section 3 above (according to it, there is no decrease below the mean value of the SAZ intensity at either day -1 or day zero, but a significant increase at day +7). In this situation, the long (as compared to the case of short geomagnetic storms) streamline of the magnetosphere by the perturbed solar wind ends approximately on the +3rd day, and the restoration of its geometrical position (expansion) to the initial one (before the beginning of the storm) begins on the +7th day. During the +7th day the magnetopause in the process of expansion slightly crosses the boundary of the initial equilibrium state, stops and begins a return movement to the equilibrium boundary, crosses it again, etc. Thus it fluctuates relative to it, stabilizing by the end of the day (the pressure in this volume changes accordingly). During this day, the SAZ increases significantly, and the sign of the magnetosphere volume recovery to the initial unperturbed state is not only the return to the initial state of the intensity of the quiet ring current, but also the pattern of the magnetospheric tail currents flow. From Fig. 6 also shows that the distribution of earthquake epicenters is already more global in nature, although they are still more numerous within the near-equatorial seismic belt.

To summarize:

a) as one of the possible physical mechanisms explaining some variations of the SAZ during strong magnetic storms, in our schematic representation is such a factor as the rate of compression (and subsequent expansion to the initial state) of the entire magnetosphere volume under the influence of the time-varying solar wind flow around the Earth's magnetosphere, which leads to pressure changes near the Earth's surface and decrease/increase of the SAZ;

b) the interaction (attraction/repulsion) of three-dimensional current systems of the magnetosphere (mainly the ring current) with the internal currents of the Earth's liquid core, caused by the Ampere force changing sharply and strongly (approximately 10 times in magnitude) during strong geomagnetic storms is too insignificant in magnitude to directly affect the observed increase in the CA3;

c) the Ampere force acting on the intensifying telluric currents during a strong magnetic storm from the side of the geomagnetic field can be a trigger of a crustal earthquake, if the physical model proposed in [Trenkin, 2015] is valid. According to this model, due to the decrease in electrical resistivity, a significant part of the electrotelluric current will flow along the contour that partially or completely includes the region of the forthcoming macrofracture.

We would like to note here that our proposed scenario of activation of the global SAZ by long geomagnetic storms with a gradual onset fits well in time with the result of earthquake prediction using the empirical formula proposed in [Doda et al., 2013] (see in detail formula (1) on p. 551 of that work and the commentary to it):

$$d_* = d_s + [(14 \vee 21) \pm 2] + 27n,$$

here d_* are the probable dates of earthquakes; d_s is the date of the geoeffective solar event causing geomagnetic disturbances on Earth; $\vee$ is a logical operation involving OR (disjunction), and the value of n (the number of Carrington cycles of the Sun) is usually 0, sometimes 1, and even more rarely 2.

Indeed, let $n = 0$, and a geoeffective solar flare accompanied by the outflow of perturbed solar wind from a coronal hole occurs on day d_s with the number 1 (i.e., $d_s = 1$), about 3.5 days later its flux (at a velocity of 500 km/s) reaches the Earth's magnetosphere (1+3.5), about a day and a half after that DST_{extr} (1+3.5+1.5) takes place, then the day with number 13 (1+3.5+1.5+7) is the first nearest day when the global SAS should increase, and it falls within the specified error ± 2 days of the above empirical formula (14-1=13). At higher perturbed solar wind speed, the +7th day after day zero of DST_{extr} in our scenario could be number 12.

It should be noted that in our consideration it turned out that the most effective, in terms of the increase in the global DST, will be geomagnetic storms with a gradual onset rather than geomagnetic storms with a sudden onset (see Fig. *4a*). At the same time, the main contribution to the increase in the SAZ on the zero day is made by short geomagnetic storms with a gradual onset ($\Delta T_{DSTextr} \leq 24$ h, see Fig. *4c*), and on the +7th day - long geomagnetic storms with a gradual onset ($\Delta T_{DSTextr} > 24$ h, see Fig. *4б*). Geomagnetic storms with a sudden onset lead to a significant decrease of the SAZ on the -1st day (the pressure increase near the Earth's surface), and the subsequent jump of the SAZ to the mean level at zero, although significant, only allows us to compensate for this decrease. Undoubtedly, the obtained conclusions should be checked on more statistics, however, it is a matter of future research in the specified direction. For the time being, we can say that the results of processing the considered observations on limited, but sufficiently large statistics, do not contradict the conducted quantitative estimates.

5. CONCLUSIONS

1. The data of the Earth's global seismic activity intensity (SAI) have been analyzed in order to reveal the possible impact of strong magnetic storms on it. The total number of strong (magnitude $M \geq 5.0$) crustal (hypocenter depth $0 \leq h \leq 60$ km) earthquakes worldwide per day (N_{EQ}) was chosen as an initial quantitative measure of the global intensity of the EAS in its analysis.

2. It was obtained that the strong geomagnetic storms with a gradual onset will be the most effective from the point of view of the increase of the global CA3. In this case, the main contribution to the increase in the SAZ on day 0 (the day of the *DST index* extremum) is made by short geomagnetic storms with a gradual onset ($\Delta T_{DST\mathrm{extr}} <$ 24 h), and on day +7 - by long geomagnetic storms with a gradual onset ($\Delta T_{DSTextr} >$ 24 h). Geomagnetic storms with a sudden onset lead to a significant decrease in DST on day -1, and the subsequent jump in DST to the mean level on day zero, although significant, only allows us to compensate for this decrease.

3. As one of the hypothetical physical mechanisms explaining some variations of the CA3 during strong magnetic storms, such a factor as the rate of compression (and subsequent expansion to the initial state) of the entire magnetosphere volume under the influence of the time-varying solar wind flow around the Earth's magnetosphere is proposed, which leads to pressure changes near the Earth's surface and a decrease/increase in the CA3.

4. The interaction (attraction/repulsion) of three-dimensional current systems of the magnetosphere (mainly the ring current) with the internal currents of the Earth's liquid core, caused by the Ampere force changing sharply and strongly (approximately 10 times in magnitude) during strong geomagnetic storms, is too insignificant in magnitude to directly affect the observed growth of the CA3.

5. The Ampere force acting on the intensifying telluric currents during a strong magnetic storm, from the side of the geomagnetic field, can be a trigger of a crustal earthquake, if the physical model proposed in [Trenkin, 2015] is valid. According to this model, due to the reduction of electrical resistance in the region of future macrofracture, a significant part of the electrotelluric current will flow along the contour that partially or fully includes the region of the forthcoming macrofracture.

ACKNOWLEDGEMENTS

The authors thank NOAA's National Geophysical Data Center (NGDC) USA, the World Data Center for Geomagnetism, Kyoto (Japan), whose geophysical and magnetic data were used in this work, and the United States Geological Survey's (USGS) Earthquake Hazards Program for providing access to earthquake data.

FUNDING

The work was supported by the Program of Fundamental Scientific Research of the State Academy of Sciences on the theme: Investigation of Solar Activity and Physical Processes in the Sun-Earth System (reg. No. 1021100714181-3).

REFERENCES

1. *Guglielmi A.V.* On the connection between earthquakes and geomagnetic disturbances // Geophysical Research. V. 21. № 2. P. 78-83. 2020. https://doi.org/10.21455/gr2020.2-6

2. *Guglielmi A.V., Lavrov I.P., Sobisevich A.L.* Sudden onset of magnetic storms and earthquakes // Solar-Terrestrial Physics. V. 1. № 1. P. 98-103. 2015.

3. *Desherevskiy A.V., Idarmachev Sh.G.* Adaptation of the superimposed epoch method for signals with irregular observation schedule // Seismic Instruments. V. 60. № 1. P. 5-24. 2024. https://doi.org/10.21455/si2024.1-1

4. *Doda L.N., Natyaganov V.L., Stepanov I.V.* Empirical scheme of short-term earthquake forecasting (in Russian) // DAN. V. 453. № 5. P. 551-557. 2013. https://doi.org/10.7868/S0869565213350144

5. *Zakrzhevskaya N.A., Sobolev G.A.* Influence of magnetic storms with sudden onset on seismicity in different regions // Volcanology and Seismology. No. 3. P. 63-75. 2004.

6. *Ivanov K.G., Semenov I.H.* Sudden increases of the atmospheric pressure on the Earth surface during geomagnetic disturbances (in Russian) // Geomagnetism and Aeronomy. V. 30. № 2. P. 329-332. 1990.

7. *Kalegaev V.V., Vlasova N.A., Peng J.* Dynamics of the magnetosphere during geomagnetic storms 21-22.I.2005 and 14-15.XII.2006 // Space Research. V. 53. № 2. P. 105-117. 2015. https://doi.org/10.7868/S002342061502003X

8. *Kalegaev V.V., Nazarkov I.S.* Dynamics of the magnetosphere during the storm 14.02.09 // Bulletin of Moscow University. Ser. 3. Physics. Astronomy. No. 3. P. 54-60. 2016.

9. *Kozyreva V.A., Pilipenko V.A.* On the relationship between geomagnetic disturbance and seismic activity for the Alaska region // Geophysical Research. V. 21. № 1. P. 33-49. 2020. https://doi.org/10.21455/gr2020.1-3

10. *Levin B.V., Sasorova E.V., Domansky A.V.* Properties of "critical latitudes", rotation variations and seismicity of the Earth // Vestnik DVO RAS. № 3. P. 3-8. 2013.

11. *Morozova A.L., Pudovkin M.I.* Atmospheric pressure variations during SPS and Forbush decreases of GCR for different climatic zones / Proceedings of the conference "The Sun in the epoch of magnetic field sign change". May 28 - June 1, 2001, GAO, Pulkovo, St. Petersburg. P. 297-304. 2001.

12. *Obridko V.N., Kanonidi H.D., Mitrofanova T.A., Shelting B.D.* Solar activity and geomagnetic disturbances // Geomagnetism and Aeronomy. V. 53. № 2. P. 157-166. 2013.

13. *Sobolev G.A., Shestopalov I.P., Kharin E.P.* Geoeffective solar flares and seismic activity of the Earth // Physics of the Earth. № 7. P. 85-90. 1998.

14. *Sobolev G.A., Zakrzhevskaya N.A., Kharin E.P.* About the connection of seismicity with magnetic storms (in Russian) // Physics of the Earth. № 11. P. 62-72. 2001.
15. *Sobolev G.A., Zakrzhevskaya N.A., Migunov I.N., Sobolev D.G., Boyko A.N.* Influence of magnetic storms on the low-frequency seismic noise (in Russian) // Physics of the Earth. № 3. P. 3-28. 2020. https://doi.org/10.31857/S0002333720030096
16. *Sobolev G.A.* Impact of a magnetic storm on tectonic deformations and coastal effect // Volcanology and Seismology. No. 2. P. 11-28. 2021. https://doi.org/10.31857/S0203030621020061
17. *Sytinsky A.D.* About the Earth seismicity connection with the solar activity (in Russian) // Uspekhi physicheskikh nauki. V. 111. № 2. P. 367-369. 1973. https://doi.org/10.3367/UFNr.0111.197310i.0367
18. *Sytinsky A.D.* On the connection of earthquakes with solar activity // Physics of the Earth. № 2. P. 13-30. 1989.
19. *Trenkin A.A.* Possible influence of telluric currents on seismicity of the Earth crust in seismically active regions // Geomagnetism and Aeronomy. V. 55. № 1. P. 139-144. 2015. https://doi.org/10.7868/S0016794015010113
20. *Khegay V.V., Legenka A.D., Abunin A.A., Abunina M.A., Belov A.V., Gaidash S.P.* Solar activity, galactic cosmic ray variations and global seismicity of the Earth // Geomagnetism and Aeronomy. V. 62. № 1. P. 40-51. 2022a. https://doi.org/10.31857/S0016794022010102
21. *Khegay V.V., Abunin A.A., Abunina M.A., Belov A.V.* Earth seismic activity and galactic cosmic rays: global and regional characteristics in 21-24 solar activity cycles // Geomagnetism and Aeronomy. V. 62. № 5. P. 556-567. 2022б. https://doi.org/10.31857/S0016794022050054
22. *Chizhevsky A.L.* Earth Echo of Solar Storms. Moscow: Mysl, 367 p. 1976.
23. *Alexeev I.I., Kalegaev V.V., Belenkaya E.S., Bobrovnikov S.Y., Feldstein Y.I., Gromova L.I.* Dynamic model of the magnetosphere: Case study for January 9-12, 1997 // J. Geophys. Geophys. Res. -Space. V. 106. № 11. P. 25683-25694. 2001. https://doi.org/10.1029/2001JA900057
24. *Daglis I.A.* Ring Current Dynamics / Solar Dynamics and Its Effects on the Heliosphere and Earth / Space Sciences Series of ISSI. Eds. Baker D.N., Klecker B., Schwartz S.J., Schwenn R., Von Steiger R. V. 22. New York, NY: Springer. P. 183-202. 2006. https://doi.org/10.1007/978-0-387-69532-7_13
25. https: //geo.phys.spbu.ru/magnetosphere/STPpracticum2005/P3_Korovinskiy/geoeffective_str.html
26. https://wdc.kugi.kyoto-u.ac.jp/
27. https://www.izmiran.ru/magnetism/magobs/MagneticStormCatalog.html

28. http://www.kaf07.mephi.ru/eduroom/appNuCosm/L8-1.pdf

29. https://www.usgs.gov/

30. http://www.wdcb.ru/stp/geomag/geomagnetic_storms.html

31. *Loewe C.A., Prölss G.W.* Classification and mean behavior of magnetic storms // J. Geophys. Geophys. Res. -Space. 1997. V. 102. № 7. P. 14209–14213. https://doi.org/10.1029/96JA04020

32. *Mironova I.A., Aplin K.L., Arnold F., Bazilevskaya G.A., Harrison R.G., Krivolutsky A.A., Nicoll K.A., Rozanov E.V., Turunen E., Usoskin I.G.* Energetic particle influence on the Earth's atmosphere //Space Sci. Rev. V. 194. № 1-4. P. 1-96. 2015. https://doi.org/10.1007/s11214-015-0185-4

FIGURE CAPTIONS

Fig. 1. Ensemble averaged values$\langle N_{EQ} \rangle$ (solid lines with dots) for the interval of 17 days obtained by the method of superposition of "epochs", with the zero day taken as the one in which the minimum value of the *DST-index* is reached. (*a*) $\langle N_{EQ} \rangle$ for the ensemble of all selected 128 geomagnetic storms (*128MS*); (*b*) $\langle N_{EQ} \rangle$ for the group of 86 geomagnetic storms with sudden onset (*86MS*$_{SC}$) included in this ensemble; (*c*) $\langle N_{EQ} \rangle$ for another group of 42 geomagnetic storms with gradual onset (*42MS*$_{GRAD}$) included in the full ensemble. Solid straight lines in the panels indicate the mean values (MEAN$\langle N_{EQ} \rangle$) over the indicated time interval, and dotted straight lines indicate the scatter bands of MEAN$\langle N_{EQ} \rangle \pm 2\sigma$, where σ is the standard (standard deviation). The solid "circles" in the figure show the exit of the values $\langle N_{EQ} \rangle$ outside the scatter band, and the "circle" given by the dashed line is for the value $\langle N_{EQ} \rangle$, approaching the upper limit of the scatter as close as possible (panel *c*, day zero).

Fig. 2. Same as Fig. 1 (panel *b*), but with a resolution of 1 hour on the time interval from day -2 to day +2.

Fig. 3. Same as Fig. 1 (panel *b*), but already for the array of geomagnetic storms $60MS_{SC}$, for which $\Delta T_{DSTextr} \leq 24$ h (i.e., 60 MS_{SC} out of a set of 86 MS_{SC}).

Fig. 4. Same as Fig. 1, but for the full $42MS_{GRAD}$ array (panel *a*) and the constituent arrays of group I (19 storms for which $\Delta T_{DSTextr} > 24$ h, panel *b*) and group II (23 storms for which $\Delta T_{DSTextr} \leq 24$ h, panel *c*).

Fig. 5. Geographic positions (circles) of earthquake epicenters of all earthquakes on day zero for the array of short geomagnetic storms with gradual onset ($23MS_{GRAD}$, $\Delta T_{DSTextr} \leq 24$ h).

Fig. 6. Same as Fig. 5, but only for long magnetic storms with gradual onset ($19MS_{GRAD}$, $\Delta T_{DSTextr} > 24$ h) on day +7, the SAZ for which is shown in panel (*b*) of Fig. 4 in section 3 above.

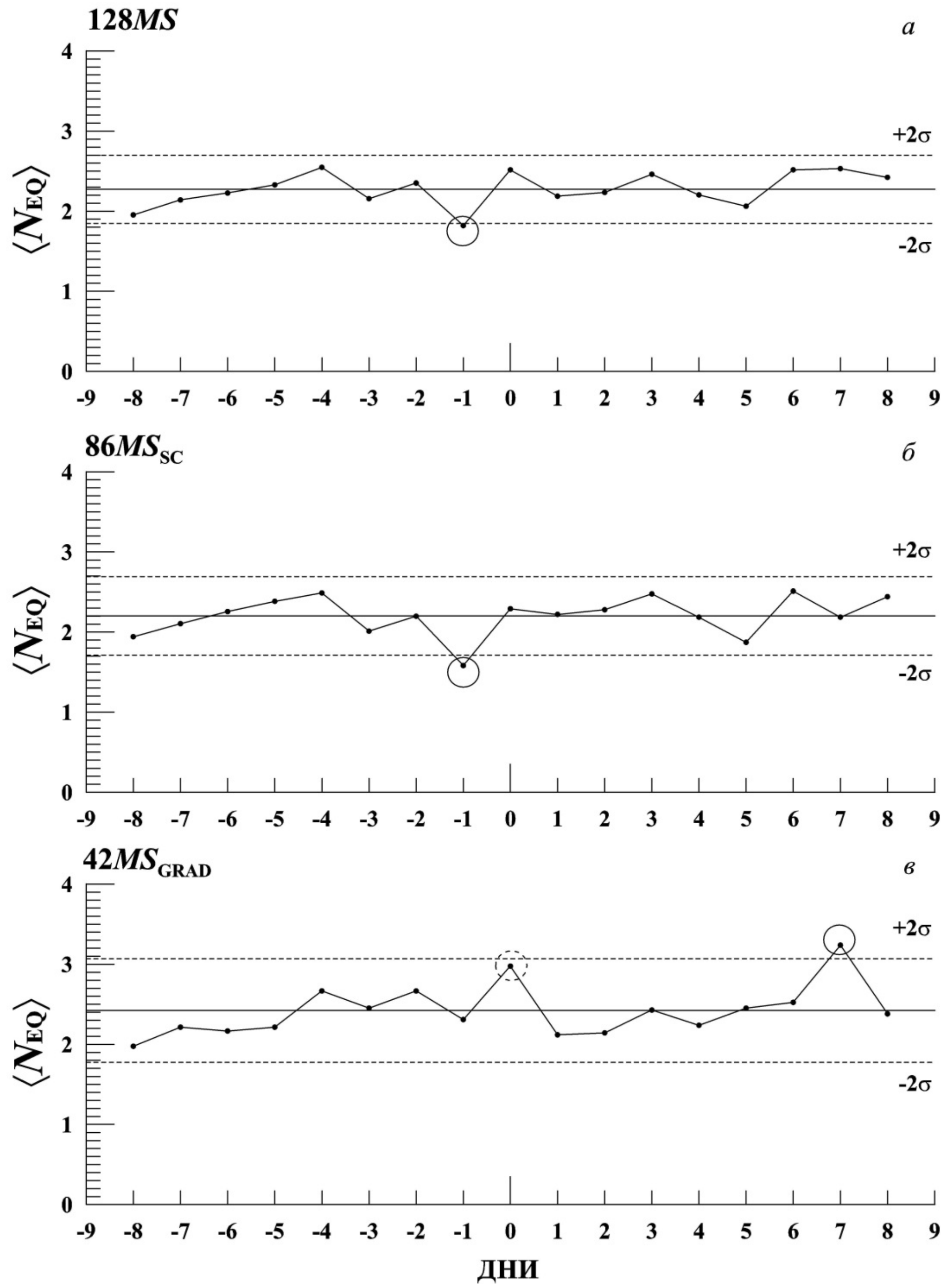

Fig. 1.

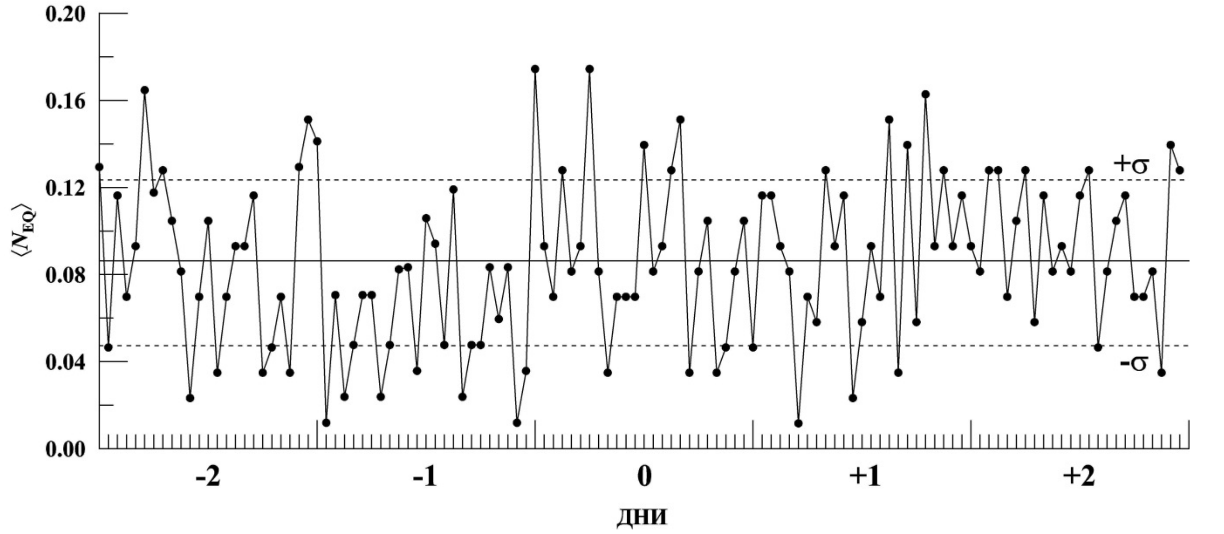
0.20
0.16
0.12
0.08
0.04
0.00
⟨N_EQ⟩
+σ
-σ
-2
-1
0
+1
+2
ДНИ

Fig. 2.

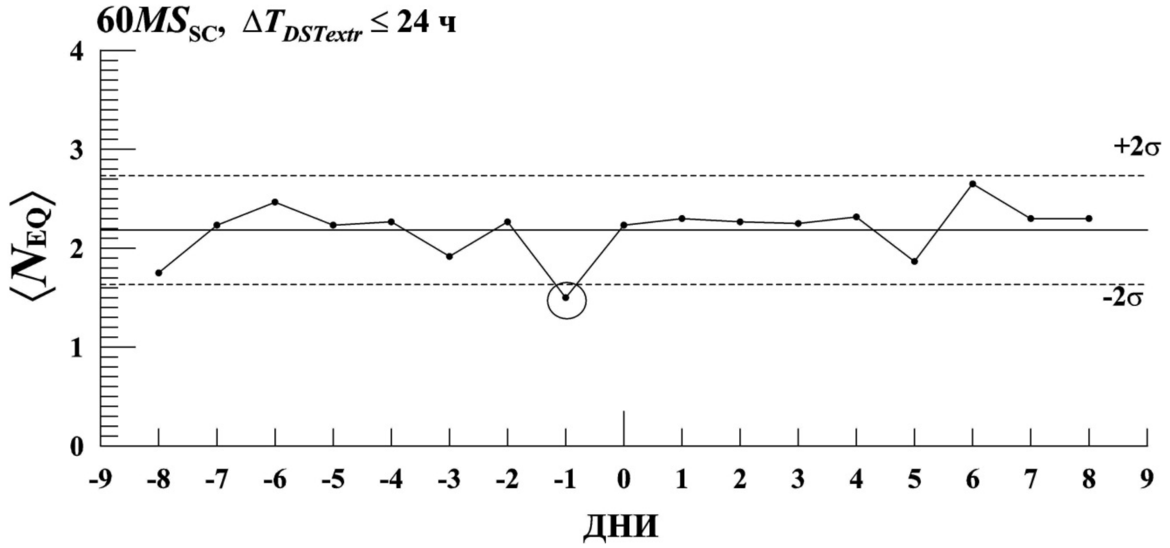
60MS_SC, ΔT_DSTextr ≤ 24 ч
4
3
2
1
0
⟨N_EQ⟩
+2σ
-2σ
-9 -8 -7 -6 -5 -4 -3 -2 -1 0 1 2 3 4 5 6 7 8 9
ДНИ

Fig. 3.

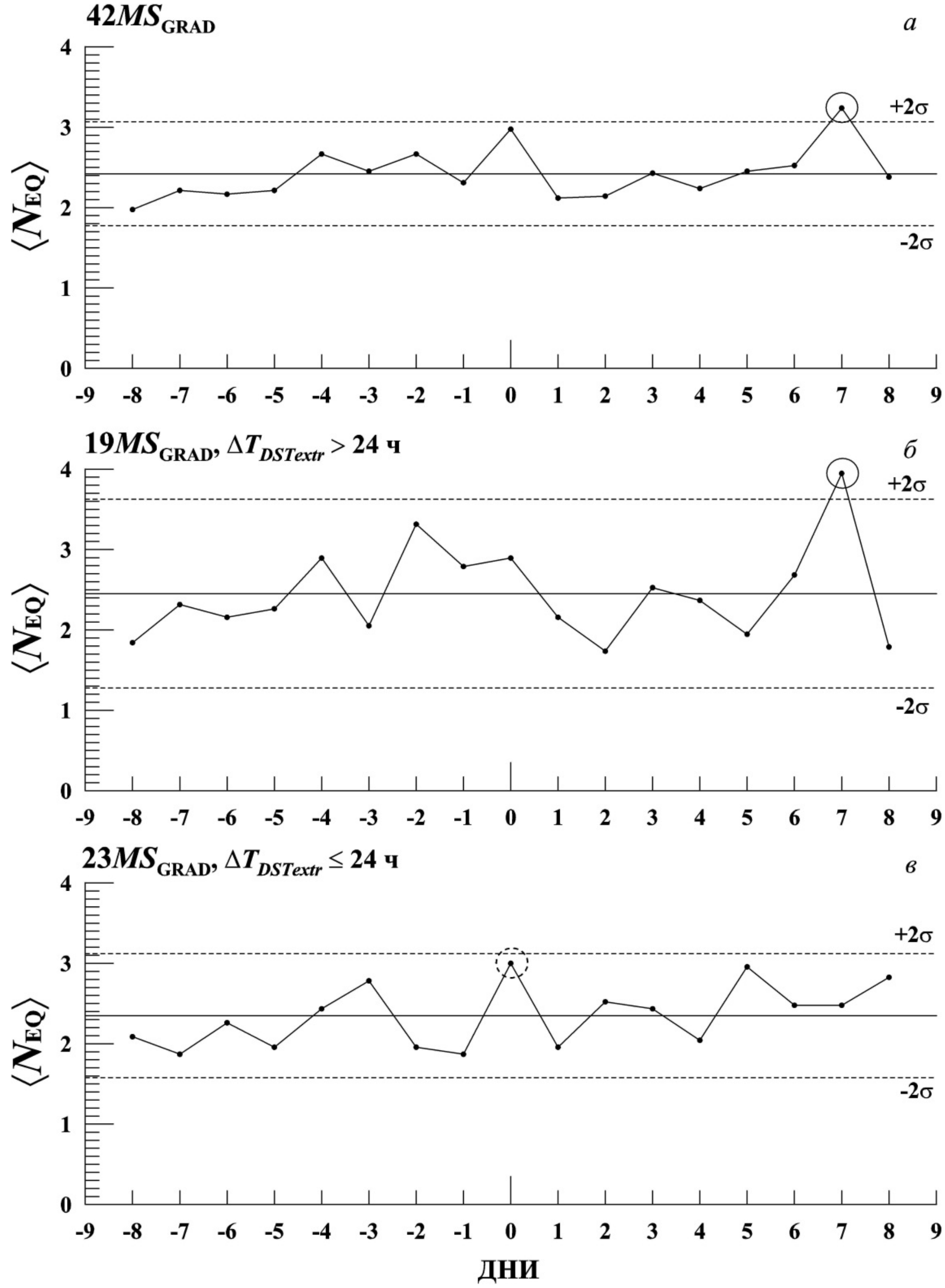

$42MS_{\mathrm{GRAD}}$
а
+2σ
-2σ
$\langle N_{\mathrm{EQ}} \rangle$
$19MS_{\mathrm{GRAD}}$, $\Delta T_{DSTextr} > 24$ ч
б
+2σ
-2σ
$\langle N_{\mathrm{EQ}} \rangle$
$23MS_{\mathrm{GRAD}}$, $\Delta T_{DSTextr} \leq 24$ ч
в
+2σ
-2σ
$\langle N_{\mathrm{EQ}} \rangle$
ДНИ

Fig. 4.

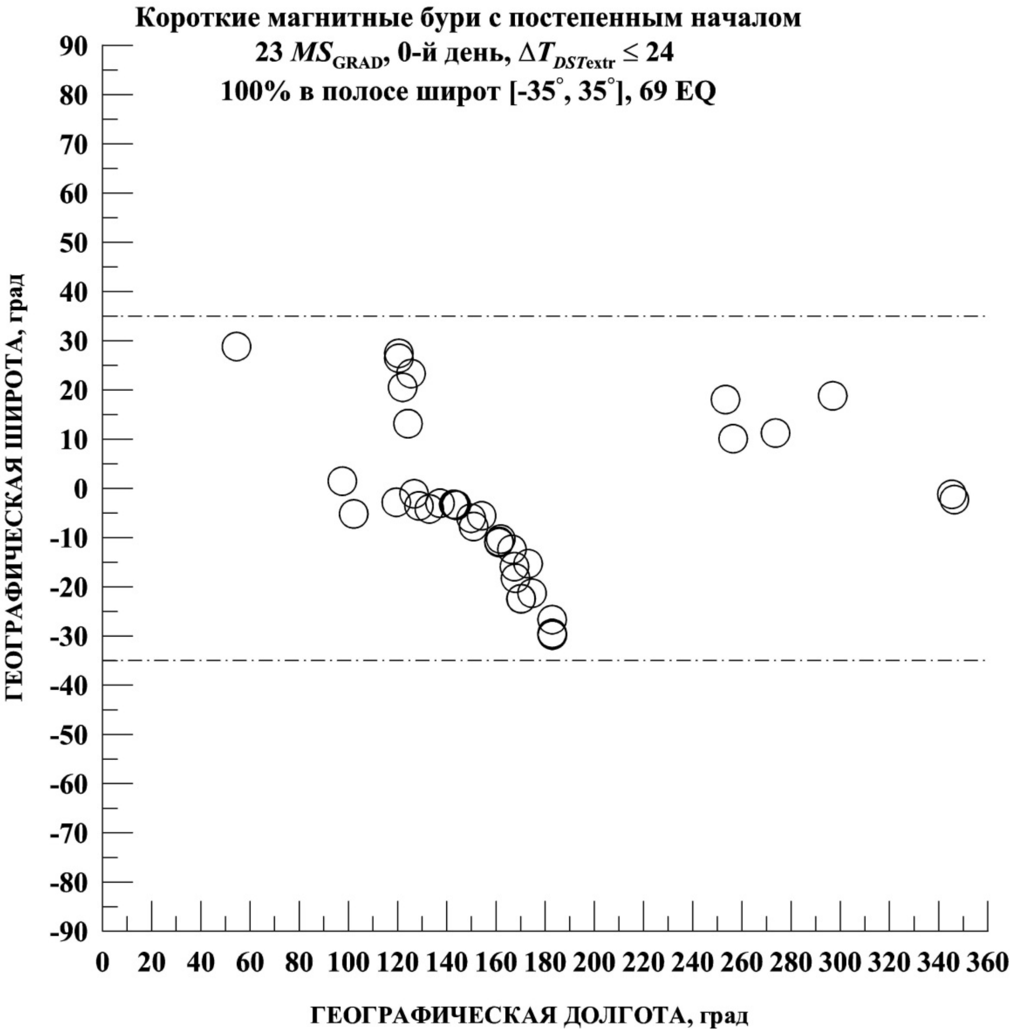
Короткие магнитные бури с постепенным началом
23 MSGRAD, 0-й день, ΔTDSTextr ≤ 24
100% в полосе широт [-35°, 35°], 69 EQ
ГЕОГРАФИЧЕСКАЯ ШИРОТА, град
ГЕОГРАФИЧЕСКАЯ ДОЛГОТА, град
90
80
70
60
50
40
30
20
10
0
-10
-20
-30
-40
-50
-60
-70
-80
-90
0 20 40 60 80 100 120 140 160 180 200 220 240 260 280 300 320 340 360

Fig. 5.

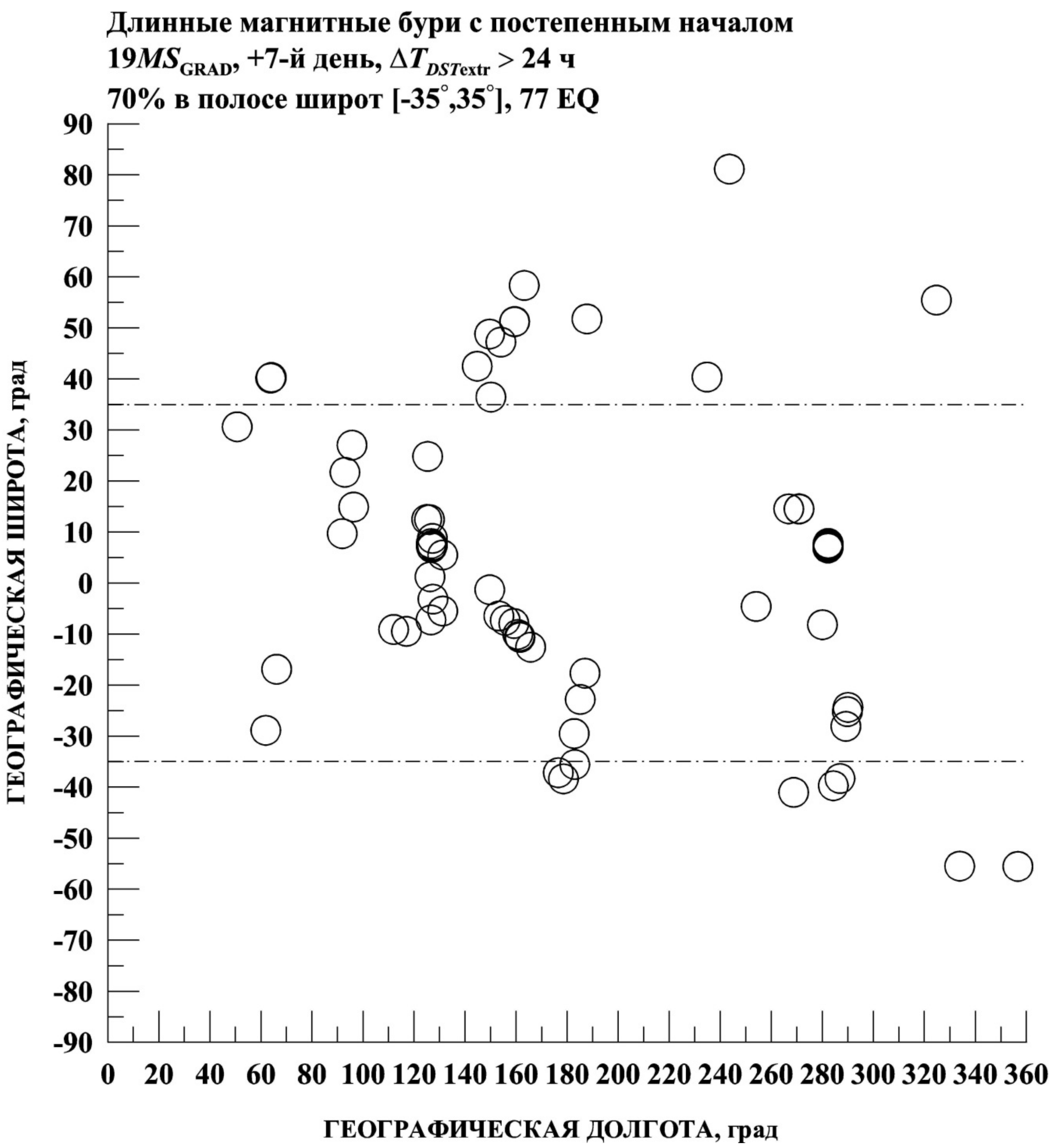

Длинные магнитные бури с постепенным началом
19MS GRAD, +7-й день, ΔT DSTextr > 24 ч
70% в полосе широт [-35°,35°], 77 EQ
90
80
70
60
50
40
30
20
10
0
-10
-20
-30
-40
-50
-60
-70
-80
-90
ГЕОГРАФИЧЕСКАЯ ШИРОТА, град
0 20 40 60 80 100 120 140 160 180 200 220 240 260 280 300 320 340 360
ГЕОГРАФИЧЕСКАЯ ДОЛГОТА, град

Fig. 6.